

# Predicting radial-velocity jitter induced by stellar oscillations based on *Kepler* data

Jie Yu,<sup>1,2</sup>★ Daniel Huber,<sup>3,1,4,2</sup> Timothy R. Bedding<sup>1,2</sup> and Dennis Stello<sup>5,1,2</sup>

<sup>1</sup>*Sydney Institute for Astronomy (SIfA), School of Physics, University of Sydney, NSW 2006, Australia*

<sup>2</sup>*Stellar Astrophysics Centre, Department of Physics and Astronomy, Aarhus University, Ny Munkegade 120, DK-8000 Aarhus C, Denmark*

<sup>3</sup>*Institute for Astronomy, University of Hawai‘i, 2680 Wood-lawn Drive, Honolulu, HI 96822, USA*

<sup>4</sup>*SETI Institute, 189 Bernardo Avenue, Mountain View, CA 94043, USA*

<sup>5</sup>*School of Physics, University of New South Wales, NSW 2052, Australia*

Accepted XXX. Received YYY; in original form ZZZ

## ABSTRACT

Radial-velocity jitter due to intrinsic stellar variability introduces challenges when characterizing exoplanet systems, particularly when studying small (sub-Neptune-sized) planets orbiting solar-type stars. In this Letter we predicted for dwarfs and giants the jitter due to stellar oscillations, which in velocity have much larger amplitudes than noise introduced by granulation. We then fitted the jitter in terms of the following sets of stellar parameters: (1) Luminosity, mass, and effective temperature: the fit returns precisions (i.e., standard deviations of fractional residuals) of 17.9% and 27.1% for dwarfs and giants, respectively. (2) Luminosity, effective temperature, and surface gravity: The precisions are the same as using the previous parameter set. (3) Surface gravity and effective temperature: we obtain a precision of 22.6% for dwarfs and 27.1% for giants. (4): Luminosity and effective temperature: the precision is 47.8% for dwarfs and 27.5% for giants. Our method will be valuable for anticipating the radial-velocity stellar noise level of exoplanet host stars to be found by the *TESS* and *PLATO* space missions, and thus can be useful for their follow-up spectroscopic observations. We provide publicly available code (<https://github.com/Jieyu126/Jitter>) to set a prior for the jitter term as a component when modeling the Keplerian orbits of the exoplanets.

**Key words:** techniques: radial velocities—planetary systems—stars: oscillations—methods: observational

## 1 INTRODUCTION

The radial velocity (RV) technique has been widely used to discover exoplanets and to confirm exoplanets detected in transit surveys (see Fischer et al. 2016; Wright 2017, for recent reviews). However, RV jitter from the host stars leads to challenges, particularly, when studying the exoplanetary signals of small (sub-Neptune-sized) planets that are expected to be detected by space-based transit missions such as *TESS* (Ricker et al. 2014) and *PLATO* (Rauer et al. 2014). Several methods have been developed to mitigate effects of stellar RV jitter, including the de-correlation magnetic activity indices (Saar et al. 1998; Isaacson & Fischer 2010), time-averaging of rapid oscillations (Dumusque et al. 2011), and modeling correlated stellar noise using Gaussian Processes (Haywood et al. 2014; Rajpaul et al. 2015) including simultaneous photometric observations (Grunblatt et al. 2015; Giguere et al. 2016). However, as of yet there are only few quantitative tools to predict the expected level of RV

jitter for a given star, which is critical to planning and prioritizing spectroscopic follow-up observations of transiting planets.

The RV jitter mainly comes from four sources: stellar oscillations, granulation (super-granulation), short-term activity from stellar rotation, and long-term activity caused by magnetic cycles (see Dumusque 2016; Dumusque et al. 2017, and references therein). For dwarfs, the oscillations and granulation have timescales on the order of minutes, while the short- and long-term activity has a longer timescale, typically greater than tens of days. In this study, we will quantify the short-timescale jitter caused by the stellar oscillations in terms of fundamental stellar properties for a wide range of evolutionary states. We emphasize that, unlike in photometry, granulation in velocity has much lower amplitude than the oscillations (Bedding & Kjeldsen 2006), and hence the results presented here can be used to predict RV jitter over a wide range of stars.

Relatively few stars so far have RV data with sufficient cadence to do seismology, so it is difficult to calibrate a RV jitter scaling relation as a function of stellar parameters. Fortunately, analysis of photometric time series can shed light on the RV jitter (Aigrain et al. 2012; Bastien et al. 2014). The *Kepler* photometric time se-

★ E-mail: jiyu9229@uni.sydney.edu.au (JY)

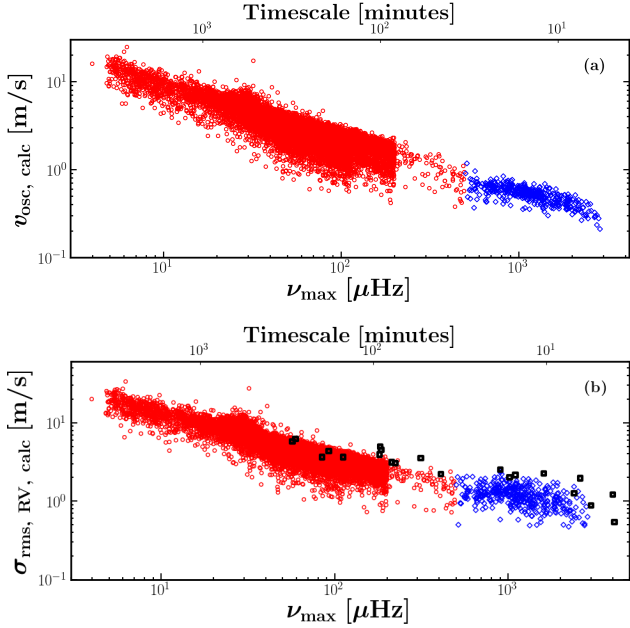


**Figure 1.** (a) RV oscillation amplitude and (b) RV jitter due to stellar oscillations. In each panel, the bottom horizontal axis is  $\nu_{\max}$ , while the top horizontal axis is the typical oscillation period (the reciprocal of  $\nu_{\max}$ ). The calculated values with different colors are separated with  $\nu_{\max} = 500 \mu\text{Hz}$ , used for the subsequent model fitting. An over-density bump at  $\nu_{\max} \sim 30 \mu\text{Hz}$  arises from red clump stars.

ries have been widely explored to study the stellar oscillations in dwarfs and giants (see a review by [Chaplin & Miglio 2013](#)). [Kjeldsen & Bedding \(1995\)](#) proposed that the spectroscopic and photometric oscillation amplitudes are convertible between each other. Moreover, it has been widely demonstrated that asteroseismology is able to provide accurate estimates of stellar parameters, based on photometric data sets (see [Chaplin & Miglio 2013](#); [Hekker & Christensen-Dalsgaard 2017](#), for reviews). These facts suggest that asteroseismic analyses on the photometric time series allow us to estimate the RV jitter in terms of stellar parameters.

In this Letter, we provide simple relations to predict the RV jitter from stellar parameters, luminosity, mass, effective temperature, and surface gravity. We also provide public code for implementing these predictions.

## 2 METHOD AND DATA

The two quantities we seek to predict are the RV oscillation amplitude,  $v_{\text{osc}}$ , and RV jitter,  $\sigma_{\text{rms, RV}}$ . It is important to keep in mind that the granulation background in RV is much lower than in photometry ([Bedding & Kjeldsen 2006](#)). Therefore, we cannot simply convert the jitter from the photometric time series to its counterpart in the RV time series. Instead, we must first subtract the contributions from granulation and photon noise. This is done most easily by working with the Fourier power spectrum.

First, we calculated the photometric oscillation amplitude,  $A_{\lambda}$ , which was then converted to the RV amplitude,  $v_{\text{osc}}$ . Specifically, the quantity  $A_{\lambda}$  was defined as the oscillation amplitude per radial

**Table 1.** Fitted parameters and the uncertainties of Equations 5, 6, and 7 for the photometric oscillation amplitude,  $A_{\lambda}$ , RV oscillation amplitude,  $v_{\text{osc}}$ , photometric stellar jitter,  $\sigma_{\text{rms, phot}}$ , and RV stellar jitter  $\sigma_{\text{rms, RV}}$ .

Giants, model: $F = F(L, M, T_{\text{eff}})$ , Equation 5					
Parameter	$\alpha$ [m/s]	$\beta$	$\gamma$	$\delta$	$\epsilon$
$A_{\lambda}$	$7.34 \pm 0.07$	$0.58 \pm 0.01$	$-1.33 \pm 0.01$	$-3.50 \pm 0.04$	-
$v_{\text{osc}}$	$0.31 \pm 0.01$	$0.60 \pm 0.01$	$-1.32 \pm 0.01$	$-2.10 \pm 0.04$	-
$\sigma_{\text{rms, phot}}$	$11.65 \pm 0.11$	$0.58 \pm 0.01$	$-1.14 \pm 0.01$	$-3.33 \pm 0.03$	-
$\sigma_{\text{rms, RV}}$	$0.58 \pm 0.01$	$0.59 \pm 0.01$	$-1.15 \pm 0.01$	$-1.55 \pm 0.03$	-

Giants, model: $F = F(L, T_{\text{eff}}, g)$ , Equation 6					
Parameter	$\alpha$ [m/s]	$\beta$	$\gamma$	$\delta$	$\epsilon$
$A_{\lambda}$	$7.30 \pm 0.07$	$-0.75 \pm 0.01$	-	$1.82 \pm 0.05$	$-1.33 \pm 0.01$
$v_{\text{osc}}$	$0.31 \pm 0.01$	$-0.72 \pm 0.01$	-	$3.20 \pm 0.05$	$-1.32 \pm 0.01$
$\sigma_{\text{rms, phot}}$	$11.59 \pm 0.11$	$-0.56 \pm 0.01$	-	$1.21 \pm 0.04$	$-1.14 \pm 0.01$
$\sigma_{\text{rms, RV}}$	$0.58 \pm 0.01$	$-0.56 \pm 0.01$	-	$3.04 \pm 0.04$	$-1.15 \pm 0.01$

Giants, model: $F = F(T_{\text{eff}}, g)$ , Equation 7					
Parameter	$\alpha$ [m/s]	$\beta$	$\gamma$	$\delta$	$\epsilon$
$A_{\lambda}$	$4.05 \pm 0.06$	-	-	$-2.15 \pm 0.06$	$-0.77 \pm 0.06$
$v_{\text{osc}}$	$0.13 \pm 0.01$	-	-	$-0.76 \pm 0.06$	$-0.63 \pm 0.06$
$\sigma_{\text{rms, phot}}$	$7.53 \pm 0.09$	-	-	$-1.59 \pm 0.05$	$-0.45 \pm 0.09$
$\sigma_{\text{rms, RV}}$	$0.34 \pm 0.01$	-	-	$0.16 \pm 0.05$	$-0.45 \pm 0.09$

Giants, model: $F = F(L, T_{\text{eff}})$ , Equation 8					
Parameter	$\alpha$ [m/s]	$\beta$	$\gamma$	$\delta$	$\epsilon$
$A_{\lambda}$	$6.15 \pm 0.13$	$0.33 \pm 0.01$	-	$-0.77 \pm 0.06$	-
$v_{\text{osc}}$	$0.19 \pm 0.01$	$0.37 \pm 0.01$	-	$-0.63 \pm 0.06$	-
$\sigma_{\text{rms, phot}}$	$10.82 \pm 0.21$	$0.37 \pm 0.01$	-	$-0.45 \pm 0.09$	-
$\sigma_{\text{rms, RV}}$	$0.46 \pm 0.01$	$0.39 \pm 0.01$	-	$-0.45 \pm 0.09$	-

Dwarfs & subgiants, model: $F = F(L, M, T_{\text{eff}})$ , Equation 5					
Parameter	Model	$\alpha$ [m/s]	$\beta$	$\gamma$	$\delta$
$A_{\lambda}$		$5.09 \pm 0.11$	$0.58 \pm 0.02$	$-0.77 \pm 0.06$	$-2.88 \pm 0.17$
$v_{\text{osc}}$		$0.30 \pm 0.01$	$0.50 \pm 0.02$	$-0.63 \pm 0.06$	$-0.96 \pm 0.16$
$\sigma_{\text{rms, phot}}$		$11.66 \pm 0.37$	$0.47 \pm 0.03$	$-0.45 \pm 0.09$	$-1.43 \pm 0.20$
$\sigma_{\text{rms, RV}}$		$0.63 \pm 0.02$	$0.47 \pm 0.03$	$-0.45 \pm 0.09$	$0.57 \pm 0.20$

Dwarfs & Subgiants, model: $F = F(L, T_{\text{eff}}, g)$ , Equation 6					
Parameter	$\alpha$ [m/s]	$\beta$	$\gamma$	$\delta$	$\epsilon$
$A_{\lambda}$	$5.08 \pm 0.11$	$-0.19 \pm 0.05$	-	$0.20 \pm 0.35$	$-0.77 \pm 0.06$
$v_{\text{osc}}$	$0.30 \pm 0.01$	$-0.13 \pm 0.05$	-	$1.57 \pm 0.35$	$-0.63 \pm 0.06$
$\sigma_{\text{rms, phot}}$	$11.64 \pm 0.37$	$0.01 \pm 0.07$	-	$0.39 \pm 0.47$	$-0.45 \pm 0.09$
$\sigma_{\text{rms, RV}}$	$0.63 \pm 0.02$	$0.01 \pm 0.07$	-	$2.38 \pm 0.47$	$-0.45 \pm 0.09$

Dwarfs & subgiants, model: $F = F(T_{\text{eff}}, g)$ , Equation 7					
Parameter	$\alpha$ [m/s]	$\beta$	$\gamma$	$\delta$	$\epsilon$
$A_{\lambda}$	$5.09 \pm 0.11$	-	-	$-1.05 \pm 0.15$	$-0.77 \pm 0.06$
$v_{\text{osc}}$	$0.30 \pm 0.01$	-	-	$0.73 \pm 0.15$	$-0.63 \pm 0.06$
$\sigma_{\text{rms, phot}}$	$11.63 \pm 0.37$	-	-	$0.46 \pm 0.19$	$-0.45 \pm 0.09$
$\sigma_{\text{rms, RV}}$	$0.63 \pm 0.02$	-	-	$2.46 \pm 0.20$	$-0.45 \pm 0.09$

Dwarfs & subgiants, model: $F = F(L, T_{\text{eff}})$ , Equation 8					
Parameter	$\alpha$ [m/s]	$\beta$	$\gamma$	$\delta$	$\epsilon$
$A_{\lambda}$	$5.45 \pm 0.13$	$0.41 \pm 0.02$	-	$-0.77 \pm 0.06$	-
$v_{\text{osc}}$	$0.33 \pm 0.01$	$0.34 \pm 0.02$	-	$-0.63 \pm 0.06$	-
$\sigma_{\text{rms, phot}}$	$12.17 \pm 0.38$	$0.36 \pm 0.02$	-	$-0.45 \pm 0.09$	-
$\sigma_{\text{rms, RV}}$	$0.66 \pm 0.02$	$0.36 \pm 0.02$	-	$-0.45 \pm 0.09$	-

mode in this manner:

$$A_{\lambda} = \frac{\sqrt{\frac{H_{\text{env}} \Delta \nu}{c}}}{\text{sinc}\left(\frac{\pi}{2} \frac{\nu_{\max}}{\nu_{\text{Nyq}}}\right)}, \quad (1)$$

where,  $H_{\text{env}}$  is the height of the oscillation power excess in the power spectrum,  $\Delta \nu$  is the mean large frequency separation between modes of the same angular degree and consecutive radial orders,  $c$  is the

effective number of modes per order, adopted as 3.04 (Bedding et al. 2010a; Stello et al. 2011),  $\nu_{\max}$  is the frequency of maximum oscillation power, and  $\nu_{\text{Nyq}}$  is the Nyquist frequency. Note that  $\nu_{\text{Nyq}}$  is equal to 283  $\mu\text{Hz}$  for the *Kepler* long-cadence (29.4 minutes) time series and 8333  $\mu\text{Hz}$  for the *Kepler* short-cadence (58.89 seconds) time series. The attenuation of the oscillation amplitude due to the integration of photons every long- or short-cadence interval was corrected with the sinc function (Huber et al. 2010; Murphy 2012; Chaplin et al. 2014).

From the photometric oscillation amplitude  $A_\lambda$ , we were able to obtain the RV amplitude  $\nu_{\text{osc}}$  via the relation given by Kjeldsen & Bedding (1995):

$$\nu_{\text{osc}} = (A_\lambda/20.1\text{ppm}) (\lambda/550\text{ nm}) (T_{\text{eff}}/5777\text{ K})^2 [\text{m s}^{-1}], \quad (2)$$

where  $T_{\text{eff}}$  is the effective temperature, and  $\lambda = 600\text{ nm}$  was taken as a representative wavelength for the broad bandpass of the *Kepler* telescope.

Next, we calculated the photometric jitter  $\sigma_{\text{rms, phot}}$ , which was then converted to  $\sigma_{\text{rms, RV}}$ . Following Kjeldsen & Frandsen (1992), the quantity  $\sigma_{\text{rms, phot}}$  was measured as

$$\sigma_{\text{rms, phot}} = \sqrt{\frac{\sigma_{\text{PS}} N}{4}}, \quad (3)$$

where  $\sigma_{\text{PS}}$  is the mean ‘noise’ level of oscillations (our jitter) in the power spectrum, and  $N$  is the number of data points of the time series. In practice, we calculated  $\sigma_{\text{PS}} \cdot N$  from a power-density spectrum, which is the power spectrum with its power multiplied by the effective observing time (Kjeldsen et al. 2008). We evaluated the area under the oscillation power excess that can be appropriately approximated with a Gaussian. Thus, we have

$$\sigma_{\text{PS}} \cdot N = \sqrt{\frac{\pi}{4 \ln 2}} H_{\text{env}} W, \quad (4)$$

where  $W$  is the full-width-at-half-maximum of the oscillation power excess.

To convert the calculated photometric jitter  $\sigma_{\text{rms, phot}}$  to the RV jitter  $\sigma_{\text{rms, RV}}$ , we used Equation 2 by replacing  $\nu_{\text{osc}}$  and  $A_\lambda$  with  $\sigma_{\text{rms, RV}}$  and  $\sigma_{\text{rms, phot}}$ , respectively. Note that we distinguish the *calculated* and *predicted*  $\sigma_{\text{rms, RV}}$  in this work. The former refers to the quantity we derive from Equations 2, 3, and 4, with the observables  $H_{\text{env}}$  and  $W$ , while the latter refers to the quantity we infer from a fitted model with stellar parameters (see Section 3 for more detail). This naming distinction is also applicable to three other quantities, namely  $A_\lambda$ ,  $\nu_{\text{osc}}$  and  $\sigma_{\text{rms, phot}}$ .

Thus, to calculate  $\sigma_{\text{rms, RV}}$  and  $\nu_{\text{osc}}$ , we need to know  $H_{\text{env}}$ ,  $W$ ,  $\nu_{\max}$ , and  $\Delta\nu$  for individual stars. We adopted the estimates of these global oscillation parameters from Huber et al. (2011) and Yu et al. (2018). Huber et al. (2011) measured these parameters for dwarfs and subgiants using short-cadence *Kepler* time series. Yu et al. (2018) determined these parameters for red giants with a homogeneous analysis of the full-length end-of-mission *Kepler* long-cadence data set, using the same analysis pipeline (Huber et al. 2009).

### 3 PREDICTING RV JITTER FROM STELLAR PARAMETERS

Figure 1a shows the calculated RV oscillation amplitude,  $\nu_{\text{osc}}$ , for dwarfs, subgiants, and giants, while Figure 1b shows the calculated RV jitter  $\sigma_{\text{rms, RV}}$ . This can be used to predict the RV jitter if  $\nu_{\max}$  is known. Black squares mark the measured  $\sigma_{\text{rms, RV}}$  from published

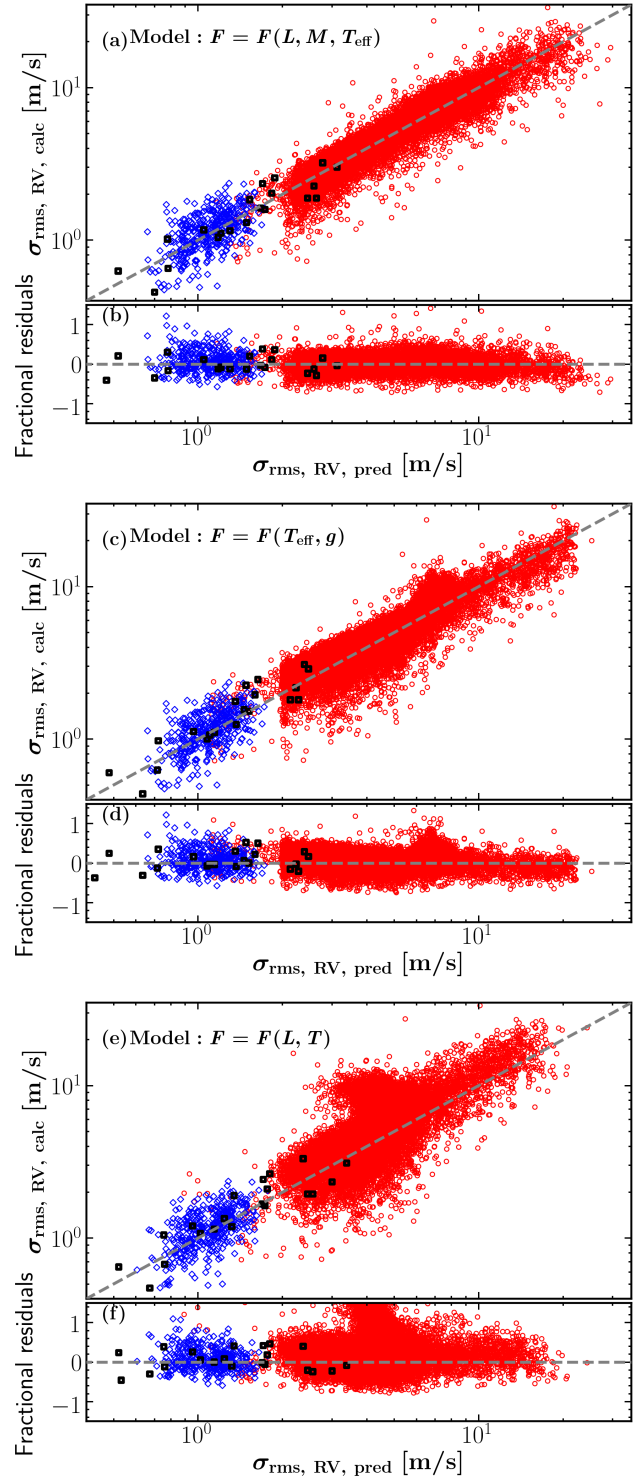


**Figure 2.** Comparison of the *calculated* with the *predicted* RV jitter  $\sigma_{\text{rms, RV}}$  (see the text for their definitions) using three models as indicated. Grey dashed lines represent perfect agreement. We separately fitted both dwarfs and subgiants (blue diamonds), and giants (red squares) using a dividing point  $\nu_{\max} = 500\text{ }\mu\text{Hz}$ , or equivalently  $\log g \sim 3.5$  dex. The bump at  $\sigma_{\text{rms, RV}} \approx 4\text{ m/s}$  is caused by red clump stars. Black squares indicate stars with long RV time series from which we computed  $\sigma_{\text{rms, RV}}$  and rescaled it to include contributions only from oscillations (see the text). Here we do not show the comparisons for  $A_\lambda$ ,  $\nu_{\text{osc}}$ , and  $\sigma_{\text{rms, phot}}$  given their almost identical features.

**Table 2.** Stellar parameters for 21 bright stars with RV time series observed by ground-based telescopes.

Star	HD	$\nu_{\max}$ [ $\mu\text{Hz}$ ]	$\sigma_{\text{rms, RV}}$ [m/s]	Ref.1 <sup>a</sup>	Luminosity $L_{\odot}$	Mass $M_{\odot}$	logg dex	$T_{\text{eff}}$ [K]	Ref.2 <sup>b</sup>
$\epsilon$ Tau	28305	56.9	5.80	Stello et al. (2017)	$75.54 \pm 1.80$	$2.40 \pm 0.36$	$2.67 \pm 0.08$	$4746 \pm 70$	Stello et al. (2017)
46 LMi	94264	59.4	6.20	Frandsen et al. (2018)	$27.42 \pm 1.38$	$1.09 \pm 0.04$	$2.674 \pm 0.013$	$4690 \pm 50$	Frandsen et al. (2018)
$\beta$ Gem	62509	84.5	3.64	Stello et al. (2017)	$36.50 \pm 1.69$	$1.73 \pm 0.27$	$2.84 \pm 0.08$	$4935 \pm 49$	Stello et al. (2017)
$\xi$ Hya	100407	90	4.37	Stello et al. (2004)	$57.65 \pm 2.39$	$2.89 \pm 0.23$	$2.883 \pm 0.032$	$4984 \pm 54$	Bruntt et al. (2010)
18 Del	199665	112	3.64	Stello et al. (2017)	$33.52 \pm 1.77$	$1.92 \pm 0.30$	$2.97 \pm 0.09$	$5076 \pm 38$	Stello et al. (2017)
HD 5608	5608	181	3.92	Stello et al. (2017)	$12.74 \pm 0.62$	$1.32 \pm 0.21$	$3.17 \pm 0.08$	$4911 \pm 51$	Stello et al. (2017)
6 Lyn	45410	183	4.94	Stello et al. (2017)	$13.74 \pm 0.73$	$1.37 \pm 0.22$	$3.18 \pm 0.09$	$4978 \pm 18$	Stello et al. (2017)
$\gamma$ Cep	222404	185	4.53	Stello et al. (2017)	$11.17 \pm 0.16$	$1.32 \pm 0.20$	$3.17 \pm 0.08$	$4764 \pm 122$	Stello et al. (2017)
$\kappa$ CrB	142091	213	3.13	Stello et al. (2017)	$11.20 \pm 0.17$	$1.40 \pm 0.21$	$3.24 \pm 0.08$	$4876 \pm 46$	Stello et al. (2017)
HD 210702	210702	223	3.06	Stello et al. (2017)	$12.33 \pm 0.52$	$1.47 \pm 0.23$	$3.26 \pm 0.09$	$5000 \pm 44$	Stello et al. (2017)
$\nu$ Ind	211998	313	3.55	Bedding & Kjeldsen (2006)	$6.28 \pm 0.23$	$1.00 \pm 0.13$	$3.432 \pm 0.035$	$5140 \pm 80$	Bruntt et al. (2010)
$\beta$ Aql	188512	410	2.22	Kjeldsen et al. (2008)	$5.73 \pm 0.19$	$1.26 \pm 0.18$	$3.525 \pm 0.036$	$4986 \pm 111$	Bruntt et al. (2010)
Procyon	61421	900	2.51	Bedding et al. (2010b)	$6.77 \pm 0.20$	$1.461 \pm 0.025$	$3.976 \pm 0.016$	$6494 \pm 48$	Bruntt et al. (2010)
$\beta$ Hyi	2151	1020	2.01	Bedding et al. (2007)	$3.41 \pm 0.13$	$1.08 \pm 0.05$	$3.955 \pm 0.018$	$5840 \pm 59$	Bruntt et al. (2010)
$\alpha$ For	20010	1100	2.14	Kjeldsen et al. (2008)	$4.87 \pm 0.16$	$1.53 \pm 0.18$	$4.003 \pm 0.033$	$6015 \pm 80$	Bruntt et al. (2010)
$\gamma$ Ser	168723	1600	2.25	Kjeldsen et al. (2008)	$3.02 \pm 0.09$	$1.30 \pm 0.15$	$4.169 \pm 0.032$	$6115 \pm 80$	Bruntt et al. (2010)
$\alpha$ Cen A	128620	2400	1.26	Butler et al. (2004)	$1.47 \pm 0.05$	$1.105 \pm 0.007$	$4.307 \pm 0.005$	$5746 \pm 50$	Bruntt et al. (2010)
$\gamma$ Pav	203608	2600	1.96	Mosser et al. (2008)	$1.52 \pm 0.05$	$1.21 \pm 0.12$	$4.397 \pm 0.022$	$5990 \pm 80$	Bruntt et al. (2010)
18 Sco	146233	3000	0.88	Bazot et al. (2011)	$1.058 \pm 0.028$	$1.02 \pm 0.03$	$4.45 \pm 0.02$	$5813 \pm 21$	Bazot et al. (2011)
$\tau$ Cet	10700	4000	1.21	Teixeira et al. (2009)	$0.47 \pm 0.02$	$0.79 \pm 0.03$	$4.533 \pm 0.018$	$5383 \pm 47$	Bruntt et al. (2010)
$\alpha$ Cen B	128621	4100	0.54	Kjeldsen et al. (2005)	$0.47 \pm 0.02$	$0.934 \pm 0.006$	$4.538 \pm 0.008$	$5140 \pm 56$	Bruntt et al. (2010)

Ref.1<sup>a</sup>: References for  $\nu_{\max}$  and time series used to calculate  $\sigma_{\text{rms, RV}}$  in this work.

Ref.2<sup>b</sup>: References for stellar parameters, luminosities, masses, logg, and  $T_{\text{eff}}$ .

RV time series for (ordered by increasing  $\nu_{\max}$ )  $\epsilon$  Tau (Stello et al. 2017), 46 LMi (Frandsen et al. 2018),  $\beta$  Gem (Stello et al. 2017),  $\xi$  Hya (Stello et al. 2004), 18 Del, HD 5608, 6 Lyn,  $\gamma$  Cep,  $\kappa$  CrB, HD 210702 (Stello et al. 2017),  $\nu$  Ind (Bedding & Kjeldsen 2006),  $\beta$  Aql (Kjeldsen et al. 2008), Procyon (Bedding et al. 2010b),  $\beta$  Hyi (Bedding et al. 2007),  $\alpha$  For,  $\gamma$  Ser (Kjeldsen et al. 2008),  $\alpha$  Cen A (Butler et al. 2004),  $\gamma$  Pav (Mosser et al. 2008), 18 Sco (Bazot et al. 2011),  $\tau$  Cet (Teixeira et al. 2009),  $\alpha$  Cen B (Kjeldsen et al. 2005). The estimates of  $\nu_{\max}$  were adopted from the corresponding literature and are given in Table 2. We can see that the measured  $\sigma_{\text{rms, RV}}$  values are slightly higher than those of *Kepler* target stars at a similar  $\nu_{\max}$ . This is due to the additional contributions from granulation at various timescales, as well as from instrumental and photon noise, in particular for dwarfs. We thus suggest to multiply the observed jitter  $\sigma_{\text{rms, RV}}$  due to the oscillations, as done in this work, by a correction factor to approximate the total RV jitter containing oscillations and granulations (see the subsequent text).

Our ultimate goal is to predict  $\sigma_{\text{rms, RV}}$  in terms of fundamental stellar properties. For this, we used four simple models. The first model is

$$F = \alpha \left( \frac{L}{L_{\odot}} \right)^{\beta} \left( \frac{M}{M_{\odot}} \right)^{\gamma} \left( \frac{T_{\text{eff}}}{T_{\text{eff}\odot}} \right)^{\delta}, \quad (5)$$

where,  $L$ ,  $M$ , and  $T_{\text{eff}}$  are luminosity, mass, and effective temperature, respectively, and  $F$  is the quantity that we seek to fit, namely one of  $\sigma_{\text{rms, RV}}$ ,  $\sigma_{\text{rms, phot}}$ ,  $A_{\lambda}$ , and  $\nu_{\text{osc}}$ , by adjusting the free parameters,  $\alpha$ ,  $\beta$ ,  $\gamma$ , and  $\delta$ . For typical exoplanet host stars, masses may not always be available, we therefore also fitted a second model by substituting the mass,  $M$ , with surface gravity,  $g$ ,

$$F = \alpha \left( \frac{L}{L_{\odot}} \right)^{\beta} \left( \frac{T_{\text{eff}}}{T_{\text{eff}\odot}} \right)^{\delta} \left( \frac{g}{g_{\odot}} \right)^{\epsilon}, \quad (6)$$

where  $\epsilon$  is a free parameter. In addition, we fitted the following two models to cater for cases where only  $T_{\text{eff}}$  and  $g$ , or  $L$  and  $T_{\text{eff}}$  are known:

$$F = \alpha \left( \frac{T_{\text{eff}}}{T_{\text{eff}\odot}} \right)^{\delta} \left( \frac{g}{g_{\odot}} \right)^{\epsilon}, \quad (7)$$

and

$$F = \alpha \left( \frac{L}{L_{\odot}} \right)^{\beta} \left( \frac{T_{\text{eff}}}{T_{\text{eff}\odot}} \right)^{\delta}. \quad (8)$$

The last model is analogous to the one used by Wright (2005), who linked the magnitude of RV jitter with  $B - V$  color and absolute magnitude of a star. In the four models, we introduced the coefficient  $\alpha$  which allows for our models to not have to pass through the solar reference point. We included luminosity in the models, given that the *Gaia* mission has provided precise parallaxes (Lindegren et al. 2018) and thus luminosities for a large number of stars observed by the *Kepler* telescope (Berger et al. 2018; Fulton & Petigura 2018).

To implement the fit, we used the non-linear least-square minimization code, *LMFIT*, with the Levenberg-Marquardt algorithm (Newville et al. 2016). We fitted separately giants and dwarfs using  $\nu_{\max} = 500 \mu\text{Hz}$ , or equivalently  $\text{logg} \sim 3.5$  dex as the dividing point. We calculated luminosities, masses, and surface gravities for the stars in Huber et al. (2011), using the well-known seismic scaling relations (Ulrich 1986; Kjeldsen & Bedding 1995). For red giants, we took the stellar parameters from Yu et al. (2018), which are based on the same relations. Effective temperatures used in this work were taken from Mathur et al. (2017).

Figure 2 shows the comparison between the calculated and predicted  $\sigma_{\text{rms, RV}}$  (See Section 2 for the definitions). We can see from Figures 2a and 2b that luminosity, mass, and temperature can be used to make quite good predictions of the RV jitter  $\sigma_{\text{rms, RV}}$  for both dwarfs and giants. The comparison returns a median fractional residual of 4.4% with a scatter of 17.9% for dwarfs, and a median fractional residual of 3.3% with a scatter of 27.1% for giants. To test the model, we computed  $\sigma_{\text{rms, RV}}$  for 21 stars, as listed in Table 2, from their real RV time series. Note that the predicted RV jitter are only from oscillations. Thus, we removed granulation contributions from the computed  $\sigma_{\text{rms, RV}}$  for the 21 stars by dividing a correction factor of 1.9. The correction factor was taken to be the median ratio between the measured  $\sigma_{\text{rms, RV}}$  from RV time series, and the predicted  $\sigma_{\text{rms, RV}}$ , using the model of Equation 5 with  $L$ ,  $M$ , and  $T_{\text{eff}}$  from Table 2. The agreement as shown in black squares is very

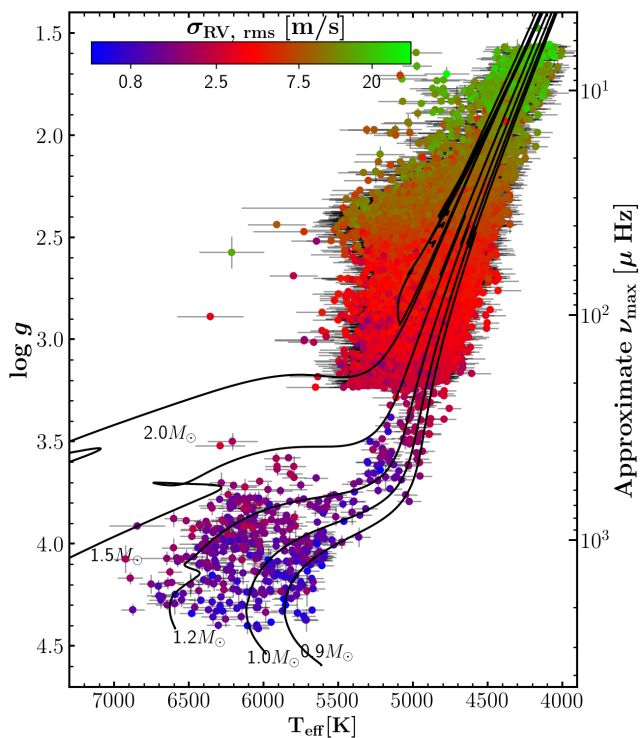


**Figure 3.**  $\log g$  vs.  $T_{\text{eff}}$  diagram color-coded by the RV jitter  $\sigma_{\text{rms, RV}}$ . Approximate  $\nu_{\text{max}}$  is labeled in the right vertical axis. The solid lines show evolutionary tracks from PARSEC (Bressan et al. 2012), with the masses from 0.8 to 2.0  $M_{\odot}$  and the metallicity  $[\text{Fe}/\text{H}] = -0.096$  equal to the median value of the whole sample.

good, with an offset of  $-1.5\%$  and a scatter of  $22.1\%$  in the fractional residuals. The model of Equation 6 gives the same fit quality with that of Equation 5, for which the comparison is not shown here.

Figures 2c and 2d show that a combination of surface gravity and effective temperature is also capable of making reasonable predictions of  $\sigma_{\text{rms, RV}}$ , with precisions of  $22.6\%$  for dwarfs and  $27.1\%$  for giants. A correction factor of 2.0 for this model is recommended. In the case where only luminosity and effective temperature are available, we still get a useful prediction of  $\sigma_{\text{rms, RV}}$  for dwarfs and subgiants ( $47.8\%$  precision) and giants ( $27.5\%$  precision), as shown in 2e and 2f. We suggest a correction factor of 1.9 for this model. The prominent feature present at  $\sigma_{\text{rms, RV}} \approx 4$  m/s is caused by red clump stars that have globally smaller masses than red-giant-branch stars at similar  $\sigma_{\text{rms, RV}}$ . We do not show the comparison figures for the photometric amplitude  $A_{\lambda}$ , RV oscillation  $\nu_{\text{osc}}$ , and photometric stellar jitter  $\sigma_{\text{rms, phot}}$ , because they exhibit similar properties to these of  $\sigma_{\text{rms, RV}}$ . We provide all the fitted parameter values and their standard deviations in Table 1.

Figure 3 shows the H-R diagram of *Kepler* targets, color-coded by the RV jitter  $\sigma_{\text{rms, RV}}$ . We observe a cutoff of star number density at  $\nu_{\text{max}} = 200$   $\mu\text{Hz}$  due to the transition from short cadence to long cadence. Typically, the RV jitter is at the level of  $\sim 0.5$  m/s in dwarfs,  $\sim 1.5$  m/s in subgiants,  $\sim 4$  m/s in low-luminosity red giants ( $\nu_{\text{max}}$  close to 100  $\mu\text{Hz}$ ),  $\sim 7$  m/s in red clump stars ( $\nu_{\text{max}}$  close to 40  $\mu\text{Hz}$ ), and  $\sim 15$  m/s in high-luminosity red giants ( $\nu_{\text{max}}$  close to 10  $\mu\text{Hz}$ ). Encouragingly, these values are consistent with observed jitter values for stars in similar evolutionary states (Johnson et al. 2010; Jones et al. 2013; Wittenmyer et al. 2016, 2017).

## 4 CONCLUSIONS

We calculated the RV jitter  $\sigma_{\text{rms, RV}}$  due to stellar oscillations using the global oscillation parameters, the height  $H_{\text{env}}$  and width  $W$  of oscillation power excess, measured with *Kepler* data. We then predicted the RV jitter in terms of stellar parameters for both dwarfs and giants. Using four sets of stellar parameters, we obtained the following precisions (i.e., standard deviations of fractional residuals):

- (i)  $L, M, T_{\text{eff}}$ : 17.9% for dwarfs and subgiants, 27.1% for giants.
- (ii)  $L, T, g$ : 17.9% for dwarfs and subgiants, 27.1% for giants.
- (iii)  $T, g$ : 22.6% for dwarfs and subgiants, 27.1% for giants.
- (iv)  $L, T$ : 47.8% for dwarfs and subgiants, 27.5% for giants.

A comparison between our calculated RV jitter  $\sigma_{\text{rms, RV}}$  and those directly computed from RV time series indicates that the predicted  $\sigma_{\text{rms, RV}}$  is globally smaller than observed in RV data. This is due to the observed  $\sigma_{\text{rms, RV}}$  values including the extra contributions from granulation, as well as photon noise and instrumental noise. We stress that the RV jitter predicted from this work are only from stellar oscillations, representing the lower limit. A correction factor is suggested to be applied to our predicted  $\sigma_{\text{rms, RV}}$ , so as to approximate the whole RV jitter including both oscillations and granulation. By calibrating on long RV time series, we recommend to increase the estimates by using a factor of 1.9 when using the models of Equation 5 and 6, and factors of 2.0 and 1.9 when using the models of Equation 7 and 8, respectively.

The predicted RV jitter  $\sigma_{\text{rms, RV}}$  can provide guidance to the follow-up spectroscopic observations for the exoplanets to be found by transit surveys, such as the *TESS* and *PLATO* space missions. They can also be used to set a prior for the jitter term as a component when modeling Keplerian orbits (e.g. Eastman et al. 2013; Fulton et al. 2018). We provide publicly available code to estimate the RV jitter  $\sigma_{\text{rms, RV}}$ .

## ACKNOWLEDGEMENTS

We gratefully acknowledge the entire *Kepler* team and everyone involved in the *Kepler* mission for making this paper possible. Funding for the *Kepler* Mission is provided by NASA’s Science Mission Directorate. D.H. acknowledges support by the National Aeronautics and Space Administration under Grant NNX14AB92G issued through the Kepler Participating Scientist Program. D.S. is the recipient of an Australian Research Council Future Fellowship (project number FT1400147).

## REFERENCES

- Aigrain S., Pont F., Zucker S., 2012, *MNRAS*, **419**, 3147  
 Bastien F. A., et al., 2014, *AJ*, **147**, 29  
 Bazot M., et al., 2011, *A&A*, **526**, L4  
 Bedding T. R., Kjeldsen H., 2006, *Mem. Soc. Astron. Italiana*, **77**, 384  
 Bedding T. R., et al., 2007, *ApJ*, **663**, 1315  
 Bedding T. R., et al., 2010a, *ApJ*, **713**, 935  
 Bedding T. R., et al., 2010b, *ApJ*, **713**, L176  
 Berger T. A., Huber D., Gaidos E., van Saders J. L., 2018, preprint, ([arXiv:1805.00231](https://arxiv.org/abs/1805.00231))  
 Bressan A., Marigo P., Girardi L., Salasnich B., Dal Cero C., Rubele S., Nanni A., 2012, *MNRAS*, **427**, 127  
 Bruntt H., et al., 2010, *MNRAS*, **405**, 1907  
 Butler R. P., Bedding T. R., Kjeldsen H., McCarthy C., O’Toole S. J., Tinney C. G., Marcy G. W., Wright J. T., 2004, *ApJ*, **600**, L75

- Chaplin W. J., Miglio A., 2013, *ARA&A*, **51**, 353
- Chaplin W. J., Elsworth Y., Davies G. R., Campante T. L., Handberg R., Miglio A., Basu S., 2014, *MNRAS*, **445**, 946
- Dumusque X., 2016, *A&A*, **593**, A5
- Dumusque X., Udry S., Lovis C., Santos N. C., Monteiro M. J. P. F. G., 2011, *A&A*, **525**, A140
- Dumusque X., et al., 2017, *A&A*, **598**, A133
- Eastman J., Gaudi B. S., Agol E., 2013, *PASP*, **125**, 83
- Fischer D. A., et al., 2016, *PASP*, **128**, 066001
- Frandsen S., et al., 2018, *A&A*, **613**, A53
- Fulton B. J., Petigura E. A., 2018, preprint, ([arXiv:1805.01453](https://arxiv.org/abs/1805.01453))
- Fulton B. J., Petigura E. A., Blunt S., Sinukoff E., 2018, *PASP*, **130**, 044504
- Giguere M. J., Fischer D. A., Zhang C. X. Y., Matthews J. M., Cameron C., Henry G. W., 2016, *ApJ*, **824**, 150
- Grunblatt S. K., Howard A. W., Haywood R. D., 2015, *ApJ*, **808**, 127
- Haywood R. D., et al., 2014, *MNRAS*, **443**, 2517
- Hekker S., Christensen-Dalsgaard J., 2017, *A&ARv*, **25**, 1
- Huber D., Stello D., Bedding T. R., Chaplin W. J., Arentoft T., Quirion P.-O., Kjeldsen H., 2009, *Communications in Asteroseismology*, **160**, 74
- Huber D., et al., 2010, *ApJ*, **723**, 1607
- Huber D., et al., 2011, *ApJ*, **743**, 143
- Isaacson H., Fischer D., 2010, *ApJ*, **725**, 875
- Johnson J. A., et al., 2010, *ApJ*, **721**, L153
- Jones M. I., Jenkins J. S., Rojo P., Melo C. H. F., Bluhm P., 2013, *A&A*, **556**, A78
- Kjeldsen H., Bedding T. R., 1995, *A&A*, **293**, 87
- Kjeldsen H., Frandsen S., 1992, *PASP*, **104**, 413
- Kjeldsen H., et al., 2005, *ApJ*, **635**, 1281
- Kjeldsen H., et al., 2008, *ApJ*, **682**, 1370
- Lindgren L., et al., 2018, preprint, ([arXiv:1804.09366](https://arxiv.org/abs/1804.09366))
- Mathur S., et al., 2017, *ApJS*, **229**, 30
- Mosser B., Deheuvels S., Michel E., Thévenin F., Dupret M. A., Samadi R., Barban C., Goupil M. J., 2008, *A&A*, **488**, 635
- Murphy S. J., 2012, *MNRAS*, **422**, 665
- Newville M., Stensitzki T., Allen D. B., Rawlik M., Ingargiola A., Nelson A., 2016, *Lmfit: Non-Linear Least-Square Minimization and Curve-Fitting for Python*, *Astrophysics Source Code Library* (ascl:1606.014)
- Rajpaul V., Aigrain S., Osborne M. A., Reece S., Roberts S., 2015, *MNRAS*, **452**, 2269
- Rauer H., et al., 2014, *Experimental Astronomy*, **38**, 249
- Ricker G. R., et al., 2014, in *Space Telescopes and Instrumentation 2014: Optical, Infrared, and Millimeter Wave*. p. 914320 ([arXiv:1406.0151](https://arxiv.org/abs/1406.0151)), doi:10.1117/12.2063489
- Saar S. H., Butler R. P., Marcy G. W., 1998, *ApJ*, **498**, L153
- Stello D., Kjeldsen H., Bedding T. R., De Ridder J., Aerts C., Carrier F., Frandsen S., 2004, *Sol. Phys.*, **220**, 207
- Stello D., et al., 2011, *ApJ*, **737**, L10
- Stello D., et al., 2017, *MNRAS*, **472**, 4110
- Teixeira T. C., et al., 2009, *A&A*, **494**, 237
- Ulrich R. K., 1986, *ApJ*, **306**, L37
- Wittenmyer R. A., Butler R. P., Wang L., Bergmann C., Salter G. S., Tinney C. G., Johnson J. A., 2016, *MNRAS*, **455**, 1398
- Wittenmyer R. A., Jones M. I., Zhao J., Marshall J. P., Butler R. P., Tinney C. G., Wang L., Johnson J. A., 2017, *AJ*, **153**, 51
- Wright J. T., 2005, *PASP*, **117**, 657
- Wright J. T., 2017, *Radial Velocities as an Exoplanet Discovery Method*. p. 4, doi:10.1007/978-3-319-30648-3\_4-1
- Yu J., Huber D., Bedding T. R., Stello D., Hon M., Murphy S. J., Khanna S., 2018, *ApJS*, **236**, 42